

## Adsorption potential of NH<sub>4</sub>Br-soaked activated carbon for cyanide removal from wastewater

Moradali Fooladvand<sup>1</sup> & Bahman Ramavandi<sup>2,3,\*</sup>

<sup>1</sup>The Persian Gulf Research Center for Tropical and Infectious Medicine, the Persian Gulf Biomedical Institute, Bushehr University of Medical Sciences, Bushehr, Iran.

<sup>2</sup>Environmental Health Engineering Department, Faculty of Health, Bushehr University of Medical Sciences, Bushehr, Iran.

<sup>3</sup>Systems Environmental Health, Oil, Gas and Energy Research Center, Bushehr University of Medical Sciences, Bushehr, Iran.

E-mail: ramavandi\_b@yahoo.com, mfooladvand39@yahoo.com

Received 2 August 2013; accepted 24 April 2014

An adsorbent has been prepared from *Populus alba* using the NH<sub>4</sub>Br-soaked activated carbon (NBAC) for cyanide removal. A series of tests have been conducted to evaluate the influence of the main parameters such as the wastewater pH, reaction time, cyanide concentration, and the NBAC quantity obtained upon the adsorption of cyanide onto NBAC. At an optimum pH of 9, more than 97% of the 200 mg/L cyanide is removed by a low NBAC dose of 1.25 mg/L during a 40 min contact time. Kinetic and isotherm modeling studies demonstrate that the experimental data best fit a pseudo-second order and Langmuir model, respectively. The maximum Langmuir adsorption capacity has been attained 102.5 mg/g at 24°C. Thermodynamic study of cyanide adsorption by NBAC has also been carried out. The efficacy of NBAC has been examined by analyzing the removal of cyanide from an industrial wastewater. Overall, NBAC is an efficient and low-cost adsorbent for the removal of different concentrations of cyanide from wastewaters.

**Keywords:** Adsorption, Cyanide, Isotherm, Kinetic, *Populus alba*, Thermodynamic.

The major sources of contamination of water bodies by cyanide are both natural phenomena (biogenesis by plants and microorganisms) and human activities (such as metal plating, electronics, photography, coal coking, plastics, chemical fertilizer, and mining)<sup>1-3</sup>. Cyanide is a very toxic compound that is included in the Comprehensive Environmental Response, Compensation, and Liability Act (CERCLA) priority list of hazardous substances<sup>3</sup> and has adverse health effects on humans and aquatic organisms<sup>4</sup>. In the case of short-term exposure, cyanide causes rapid breathing, tremors, and other neurological effects, and a long-term exposure to cyanide causes weight loss, thyroid effects, nerve damage, and death. Skin contact with liquids containing cyanide may produce irritation and sores<sup>2</sup>. Therefore, to conform to environmental regulations, wastewater containing cyanide must be treated to reduce the cyanide concentration to less than 0.2 mg/L before discharging the wastewater into the environment<sup>5,6</sup>. Several methods are available for cyanide removal, such as biological, chemical, and physical processes, as reviewed by Dash *et al.*<sup>2</sup>. In general, biological processes are preferred for

cyanide removal because of their cost effectiveness and eco-friendliness. Further, the toxic effect of cyanide at high concentration on microorganisms adversely affects the efficiency of the biodegradation processes<sup>7-9</sup>. Another option for cyanide removal is a chemical method that is currently used in some wastewater treatment plants<sup>10,11</sup>. However, this technique is unattractive because it involves the use of chemical compounds, is expensive, produces toxic residues, and does not degrade the full range of cyanide compounds<sup>3,12,13</sup>. An adsorption technique is also used for cyanide removal. These techniques are simple to operate, are not affected by the toxicity of the target pollutant(s), and do not require hazardous chemicals. Furthermore, adsorption facilitates concentrating and then recycling the adsorbate if desired.

Table 1 summarizes some of published literature<sup>7-22</sup> on cyanide removal by an adsorption process. As shown, the most common adsorbent is plain or impregnated activated carbon, which has a relatively low cyanide adsorption capacity ranging from 6.6 to 68.02 mg/g. Because of its low capacity for cyanide

Table 1 — Summary of recently published literature on cyanide adsorption by activated carbon

Adsorbent	Opt. pH	Fitted kinetic model	Fitted isotherm model	Adsorption capacity (mg/g)	Ref.
Cu-impregnated AC	10.5–11	Pseudo-second order	Langmuir	19.7	17
Ag-impregnated AC	10.5–11	Pseudo-second order	Langmuir	22.4	17
Plain AC	10.5–11	Pseudo-second order	Langmuir	29.6	17
Plain carbon	–	–	–	6.6	18
TBA-carbon	–	–	–	29.2	18
Ag-impregnated AC	>11	–	–	26.5	19
Ni-impregnated AC	>11	–	–	15.4	19
Plain AC	>11	–	–	7	19
AC	10.5	–	Freundlich	–	20
AC	10	Pseudo-second order	Koble–Corrigan	–	21
LAC	10–10.5	Pseudo-second order	Langmuir	64.1	22
FeAC	10–10.5	Pseudo-second order	Langmuir	68.02	22

removal, the production and regeneration of activated carbon is very expensive<sup>14</sup>, making it impractical for full-scale applications. Moreover, commercially available activated carbon is still considered expensive because of the use of non-renewable and relatively expensive starting materials such as coal. To make the adsorption process attractive and feasible, novel low-cost adsorbents with relatively high adsorption capacities are required. This has led to a growing research interest in the production of activated carbon from renewable and relatively cheap precursors.

In this study, an attempt has been made to use *Populus alba* as a low-cost, abundantly available, and renewable precursor for the production of activated carbon as an adsorbent for the removal of cyanide from wastewater. This tree (*P. alba*) is considered because it is fast-growing and easily found in Iran. Interestingly, it has been found that the adsorption of pollutants onto activated carbon is significantly influenced by the characteristics and the origin of the activated carbon<sup>15</sup>. Therefore, the method of carbon activation is aimed at improving the material's adsorption capability and therefore decreasing the rate of activated carbon consumption to reduce the cost of activated carbon adsorption, making it more cost effective.

Several chemicals have been used in the process of microwave-assisted activation of carbon, and the best activation has been obtained with the presence of an alkaline hydroxide such as KOH<sup>16</sup>. However, the main challenge faced by this method of microwave-assisted modification of activated carbon using metal salts is the metal compound formed during the activation process<sup>16</sup>. These metal compounds are deposited in the internal structure and pores of the adsorbent, thereby reducing its pore volume and

specific surface area. Accordingly, non-metal hydroxides might be used as an alternative chemical to activate carbon.

Therefore, the purpose of this work is to evaluate the adsorption potential of NH<sub>4</sub>Br-soaked activation of carbon (NBAC) prepared from *P. alba* wood for cyanide removal from wastewater. The impacts of operational parameters and the equilibrium, isotherm, kinetic, and thermodynamic data of the adsorption process are studied to better understand the mechanism of the cyanide adsorption onto the NBAC. For the latter, the applicability of NBAC is investigated in the case of the treatment of industrial wastewater under optimized conditions.

## Experimental Section

### Adsorbate preparation

A cyanide solution was prepared by diluting aliquots of a 1 g/L stock cyanide solution with distilled water. The stock solution was made by dissolving NaCN in distilled water. All the chemicals and reagents were of analytical grade and were used without further purification (Merck Co., Germany).

### Preparation of NBAC

*P. alba* trees, the fast-growing trees, were identified in the west of Iran. Dried *P. alba* wood was used as the base material for the preparation of activated carbon. The *P. alba* wood was collected along a river in the west of Iran. The wood was first ground using a grinder to obtain a uniform particle size of more than 0.85 mm and less than 1 mm. The resultant sieve was carbonized in a stainless steel vertical tubular reactor placed in a tube furnace at 700°C under purified nitrogen (99.9%) flow of

150 cm<sup>3</sup>/min for 2 h. The heating rate was fixed at 10°C/min. The char produced was then soaked in the NH<sub>4</sub>Br solution (the NH<sub>4</sub>Br to char ratio was 3 wt.%). The mixture was then dehydrated in an oven overnight at 105°C and then activated to a final temperature of 850°C at the heating rate of 10°C/min. Once the final temperature was reached, the nitrogen gas flow was switched to carbon dioxide and activation was conducted for 2 h. The activated carbon was then cooled to room temperature under a nitrogen flow of 150 cm<sup>3</sup>/min. Next, the activated carbon was washed with 0.1 M hydrochloric acid and then washed with distilled water until the pH of the washing solution reached 6.5-7<sup>23</sup>. Accordingly, the prepared NBAC was again sieved to obtain a particles size of less than 1 mm for use in the adsorption experiments.

#### Adsorbent characterization and analytical methods

At the beginning of the experiment, the prepared powder was characterized by evaluating the pH of zero point charge (pH<sub>zpc</sub>), specific surface area, pore volume and size, surface morphology, and surface functional groups. The specific surface area (based on the BET method) and the pore volumes were determined using a nitrogen gas adsorption analyzer (Micromeritics/Gemini-2372). The mean pore diameter was calculated using BET, and the total pore volume was calculated using the equation reported by Altener *et al.*<sup>24</sup>. The surface structure of the NBAC particles was analyzed by scanning electron microscopy (SEM) (Philips XL-30). To identify the functional groups present on the surface of the adsorbent, Fourier transform infrared (FTIR) spectra were collected between 400 and 4000 cm<sup>-1</sup> using a Nicolet spectrometer. The pH level of the samples was measured using a pH meter (Sense Ion 378, Hack). The temperature of the solutions was measured using a mercury thermometer. The concentration of the cyanide ions in the solution was measured using a titrimetric method as described in Section 4500-CN- D. of the Standard Methods<sup>25</sup>.

#### Adsorption experiments

All adsorption experiments were conducted in a routine manner by using a batch technique over several runs in 250 mL Erlenmeyer flasks. Table 2 presents the experimental runs and conditions. For each experiment, 150 mL of the cyanide solution was added to the flasks, and the test conditions were adjusted to the designated value (Table 2). Then, a

given mass of NBAC was added to the solution and the suspension was immediately shaken at 120 rpm in a shaker-incubator instrument (Pars Azma Co., Iran). Upon reaching the preset contact time for each test, the suspension was filtered using a 0.2 μm pore size filter, and the filtrate was analyzed for residual cyanide. The cyanide adsorption efficiency (RE) and the equilibrium adsorption capacity (q<sub>e</sub>) were then calculated from Eqs. (1) and (2). The pH of the artificial wastewater was adjusted to the desired level using a 0.1 N NaOH or HCl solution. The impact of variable parameters such as the wastewater pH, contact time, initial target contaminant concentration, and the adsorbent quantity was evaluated under different conditions in this research. All the experiments were conducted in triplicate to ensure the reproducibility of the results; the mean of these three measurements along with the standard deviation are given in this paper.

$$RE = \frac{C_0 - C_t}{C_0} \times 100 \quad \dots (1)$$

$$q_e = \frac{V(C_0 - C_e)}{m} \quad \dots (2)$$

## Results and Discussion

#### Adsorbent characteristics

The pH<sub>zpc</sub> of the prepared activated carbon was determined from the titration curve to be approximately 6.3, signifying a positive surface charge for a solution pH below 6.3 and a negative surface charge for a solution pH greater than 6.3. The specific BET surface area and the total pore volume (at P/P<sub>0</sub> = 0.990) of the fresh NBAC were 1034 m<sup>2</sup>/g and 0.0012 cm<sup>3</sup>/g, respectively. The greater surface area for NBAC leads to a good possibility of pollutant adsorption. The mean diameter of the pores in the fresh NBAC was found to be 1.54 nm (mesoporous structure). SEM was used for observing the NBAC morphology, and the related micrograph is shown in Fig. 1, at 500× magnification. The image of the NBAC (Fig. 1) indicates that the activated carbon surface has a porous surface. Further, Fig. 1 shows the NBAC that contains well-developed pores and has a good possibility for cyanide ions to be trapped and adsorbed into the surface of the pores.

The chemical structure of the adsorbent is of vital importance in understanding the adsorption process. The FTIR technique is an important tool to identify the characteristic functional groups. In Fig. 2, the

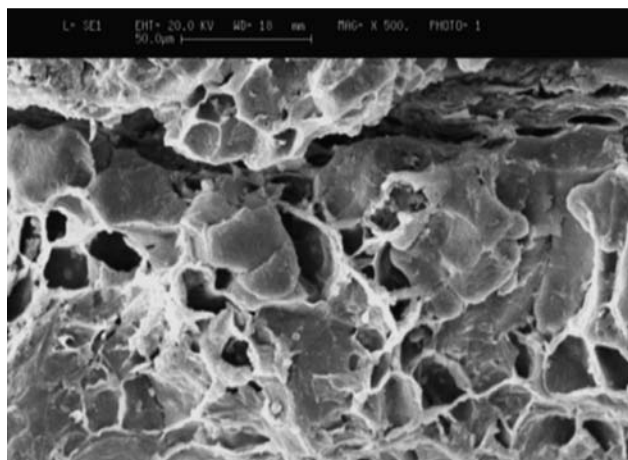


Fig. 1 — SEM micrograph of NBAC (magnifications: 500×)

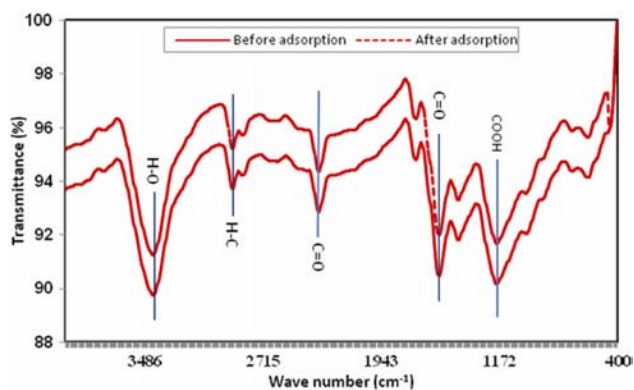


Fig. 2 — FTIR spectrum of NBAC at wave numbers from 400 to 4000  $\text{cm}^{-1}$

functional groups before and after  $\text{CN}^-$  adsorption onto NBAC and the corresponding infrared adsorption bands are shown. As shown in Fig. 2 and on the basis of the existing literature<sup>26</sup>, we know that the spectra display a number of adsorption peaks, indicating the active functional groups on the surface of NBAC. These peak shifts after adsorption indicate that the bonded -OH groups, C=O stretching, and -COOH group play a major role in the  $\text{CN}^-$  adsorption on NBAC. Therefore, a change in the -OH, -COOH, C=O, and H-C functional groups suggests that these groups are the main active groups involved in the adsorption of cyanide. The main changes in the band between 2800 and 3500  $1/\text{cm}$  after the adsorption of cyanide indicate the ion-exchange processes predominantly involved in the adsorption of cyanide by NBAC.

#### Impact of solution pH and the mechanism of adsorption

The effect of the solution pH on the removal of cyanide by NBAC was studied for the pH range of

2-12 under the conditions listed in Table 2. Since the pH of the aqueous solution affects the surface charge of the adsorbents as well as the degree of ionization and speciation of different pollutants<sup>27</sup>, in the Run 1 experiments. The results of the pH effect on cyanide removal are shown in Fig. 3. This figure clearly shows that the adsorption of cyanide is highly influenced by the solution pH: as the solution pH is increased from 2 to 9, the efficiency of cyanide removal increases from 79% to 97%. This phenomenon can be explained by the fact that the pH of the solution influences both the surface charge of the NBAC particles and the dominant species of cyanide in the solution. In another attempt, the pH of zero point charge ( $\text{pH}_{\text{zpc}}$ ) for NBAC particles is determined to be 6.3. Therefore, at a pH greater than  $\text{pH}_{\text{zpc}}$ , the surface of NBAC is negative and as reported<sup>28</sup>, the HCN is completely dissociated to free cyanide ( $\text{CN}^-$ ) and  $\text{H}^+$  at an alkaline solution pH. Because free cyanide is a nucleophilic ion, when it comes into contact with the negatively charged adsorbent, it binds with the anionic functional groups like the hydroxyl group present on the surface of the adsorbent (Fig. 2) and thereby improves adsorption<sup>2</sup>. Therefore, from this result, it can be suggested that a chemical ion exchange is the main mechanism in the adsorption of  $\text{CN}^-$  by NBAC. However, a further evaluation of the mechanism of adsorption processes and the functional groups on NBAC involved in the adsorption of cyanide is discussed in adsorbent characteristics section. The result of other research<sup>17</sup> indicated that the dominated species of cyanide in  $\text{pH} > 10$  is free cyanide, and Moussavi and coworkers<sup>29</sup> confirmed that in the case of  $\text{pH} > \text{pH}_{\text{zpc}}$ , the mechanism for cyanide adsorption is ion exchange. However, some researchers have stated that under alkaline conditions, the cyanide removal may occur through surface precipitations and chemical reactions with surface sites, complexation of  $\text{CN}^-$  with functional groups, and physical adsorption<sup>24</sup>. According to Table 1, most researchers have similarly reported attaining maximum cyanide adsorption onto different adsorbents in the case of alkaline pH.

#### Impact of NBAC quantity

Another experiment was conducted to determine the effects of NBAC quantity in the range of 0.25-2 mg/L on cyanide adsorption at an optimum pH of 9 under the conditions given in Table 2. As illustrated in Fig. 4, the removal of cyanide at a dose of 0.25 mg/L was 77.8%; removal improved to 96.4% when

Table 2 — Experimental runs and conditions for cyanide adsorption onto NBAC

Run	Purpose	Conditions				
		pH	CN <sup>-</sup> , mg/L	NBAC, mg/L	Contact time, min	Temperature, °C
1	Effect of solution pH	2-12	200	1.25	40	24
2	Effect of NBAC dosage	9	200	0.25-2	40	24
3	Effect of contact time and cyanide concentration	9	100, 200, 300	1.25	3-50	24
4	Isotherm modeling	9	50, 100, 200, 300, 400	1.25	360	24, 35, 50
5	Kinetic study	9	100, 200, 300	1.25	3-50	24
6	Thermodynamic study	9	100, 200, 300	1.25	40	24, 35, 50
7	Real wastewater treatment	8.3	112	1.25	40	24

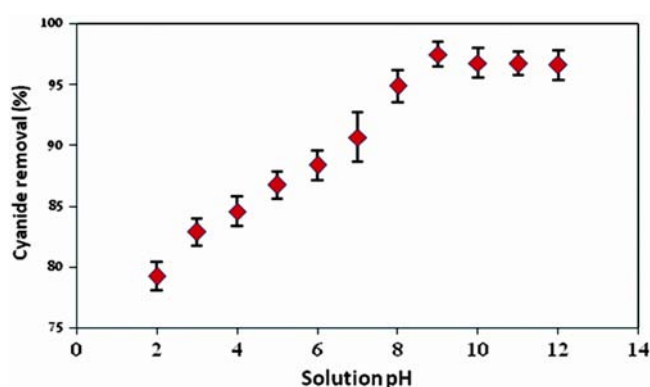


Fig. 3 — Impact of solution pH on cyanide adsorption by NBAC

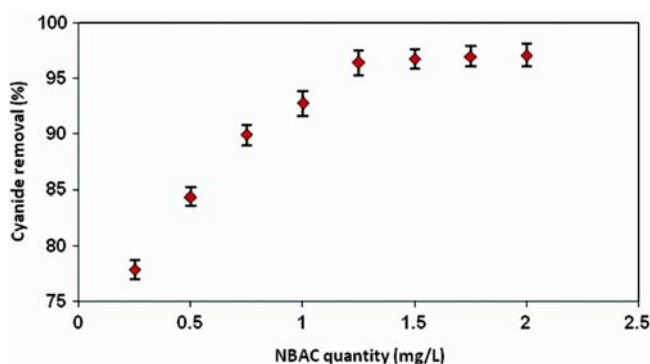


Fig. 4 — Impact of NBAC dose on cyanide adsorption by NBAC

the NBAC quantity was increased to 1.25 mg/L and remained approximately constant thereafter. Hence, the optimum dose of NBAC for the removal of cyanide can be considered to be 1.25 mg/L of NBAC for the rest of the adsorption experiments. This result is in accordance with that of other studies<sup>17,29</sup>, where an increase in CN<sup>-</sup> adsorption was observed with an increase in the concentration of the adsorbent. However, the maximum cyanide adsorption accrued at a low adsorbent dose of 1.25 mg/L, whereas Mossavi *et al.*<sup>29</sup> stated 1.5 g/L and Devici<sup>17</sup> reported 3 mg/L as the optimum dosage for maximum cyanide adsorption. The enhancement of cyanide removal as a

function of the NBAC dose to 1.25 mg/L is due to the greater availability of active exchangeable sites and to the presence of a greater surface area for adsorption. Further, it can be seen that the rate of cyanide adsorbed by NBAC did not significantly increase with an increase in the NBAC dosage from 1.25 to 2 mg/L. One plausible reason could be the overlap of active sites at higher adsorbent masses, resulting in a reduced effective surface area required for adsorption<sup>30</sup>. The achievement of a high cyanide removal percentage with a very low adsorbent dose demonstrated the high affinity and suitability of NBAC for the removal of cyanide from wastewaters.

#### Impact of contact time and cyanide concentration

The contact time between the pollutant and the adsorbent is of significant importance in the wastewater treatment by an adsorption process. A rapid adsorption of the pollutants and the establishment of equilibrium in a short period signify the efficacy of the adsorbent for its use in wastewater treatment. The effect of varying the initial cyanide concentration (100, 200, and 300 mg/L) on the adsorption efficiency was investigated under the conditions listed in Table 2. On the basis of the data plotted in Fig. 5, we concluded that the cyanide adsorption onto NBAC for all initial cyanide concentrations increased with an increase in the contact time to 30 min. In other words, after 30 min, the equilibrium for adsorption was achieved and the time required for reaching the equilibrium was independent of the initial cyanide concentrations. Devici and coworkers<sup>17</sup> showed that the cyanide adsorption onto activated carbon was very slow, whereas after 4 h, the equilibrium of the adsorption was achieved. A similar finding was reported by Behnamfard and coworkers<sup>21</sup>. The contradictory report in the existing literature can account for the methods of determining the adsorbent and adsorbent

properties such as the size and the volume of the pores. It is observed from Fig. 5 that an increase in the cyanide concentration leads to a decrease in the adsorption efficiency. This phenomenon can be described by the limitation of the available free sites for the adsorption of cyanide with increased cyanide concentration in a bulk solution for a fixed mass of adsorbent as well as by an increase in the intraparticle diffusion. Some reports related to the abovementioned phenomenon are available<sup>21,29</sup>.

Moreover, it is observed from Fig. 5 that the rate of cyanide removal is fast in the first 20 min of the contact time, and then, the process is slow. The slow rate of the final step in the CN<sup>-</sup> adsorption is considered to be the diffusion of CN<sup>-</sup> from the bulk solution to the active surface sites. This process is influenced by the concentration gradient related to the thickness of the diffusion layer, which is a function of an agitation process<sup>31</sup>. In a physical adsorption, most of the adsorbates are adsorbed within a short interval of contact time<sup>5</sup>. However, a strong chemical binding of adsorbates with an adsorbent requires a relatively long contact time for attaining equilibrium. The available adsorption results show that the uptake of the adsorbate is fast at the beginning of the contact time, and thereafter, it becomes relatively slow near the equilibrium. In between these two stages of the uptake, the rate of adsorption is found to be almost constant. This is obvious from the fact that a large number of vacant surface sites are available for adsorption during the initial stage, and after some time, the remaining vacant surface sites are difficult to occupy because of the repulsive forces between the solute molecules of the solid and the bulk phase<sup>5,31</sup>. A similar result was reported by Dash *et al.*<sup>5</sup>.

**Equilibrium adsorption and isotherm modeling**

The adsorption isotherms express how contaminants interact with the adsorbent surface materials. Therefore,

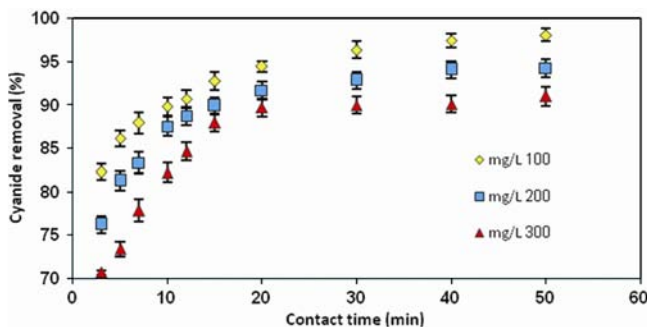


Fig. 5 — Impact of contact time and initial cyanide concentration on cyanide adsorption by NBAC

an analysis of the isotherm data is critical for determining the maximum capacity of the adsorbent, appearance of the surface properties, and optimization of the adsorption pathways, as well as for formulating an equation for an effective design of columns. Accordingly, to evaluate the cyanide adsorption capacity at different temperatures (Table 2) and its adsorption behavior onto NBAC, the obtained isotherm data were fitted by the four most commonly applied isotherms, namely Langmuir, Freundlich, Dubinin-Radushkovich (D-R), and Temkin. The linear forms of the applicable isotherm equations are given in Table 3 and in the “nomenclature” section, which describes the parameters and the constants of the fit models. Table 4 lists the parameters of the isotherms obtained by linear regression methods and

Table 3 — Linearized expressions of adsorption isotherms<sup>32,33</sup>

Isotherm	Linearized form	Plot	Parameters
Langmuir	$\frac{C_e}{q_e} = \frac{1}{k_L q_{max}} + \frac{C_e}{q_{max}}$	$\frac{C_e}{q_e}$ vs $C_e$	$q_{max} = 1/\text{slope}$ $K_L = \text{slope}/\text{intercept}$
Freundlich	$\ln q_e = \ln k_f + n^{-1} \ln C_e$	$\ln q_e$ vs $\ln C_e$	$K_F = \exp(\text{intercept})$ $n = 1/\text{slope}$
Temkin	$q_e = B_T \ln A_T + B_T \ln C_e$	$q_e$ vs $\ln C_e$	$B_T = \text{slope}$ $A_T = \exp(\text{intercept}/\text{slope})$
D-R	$\ln q_e = \ln q_m - K_{DR} E^2$	$\ln q_e$ vs $E^2$	$q_m = \exp(\text{intercept})$ $K_{DR} = -\text{slope}$

Table 4 — Information of cyanide adsorption isotherm onto NBAC

Isotherm model	Parameters	Equilibrium Temp(°C)		
		24	35	50
Langmuir	$K_L$	0.0055	0.046	0.003
	$q_{max}$	102.5	109.9	117.7
	$R_L$	0.088	0.59	0.56
	$R^2$	0.998	0.988	0.987
	RMSE	5.80	6.04	6.84
Freundlich	$K_F$	70.45	47.66	49.81
	$1/n$	0.38	0.41	0.46
	$R^2$	0.956	0.945	0.954
	RMSE	26.38	29.68	31.79
Temkin	$B_T$	7	11	14
	$A_T$	3.24	3.65	12.5
	$R^2$	0.942	0.953	0.952
	RMSE	17.43	19.27	22.73
D-R	$K_{DR}$	0.002	0.005	0.007
	$E$	15.8	10	8.5
	$R^2$	0.856	0.866	0.883
	RMSE	30.67	36.82	37.75

the calculated adsorption isotherm parameters for cyanide adsorption onto NBAC. Table 4 shows that the adsorption of cyanide onto NBAC fitted with Langmuir model has the highest value of the correlation coefficient ( $R^2$ ). Apart from the correlation coefficient, the applicability of the isotherm equations was further evaluated by comparing the residual root mean square error (RMSE)<sup>34</sup>, which can be described as follows:

$$\text{RMSE} = \sqrt{\frac{1}{n-2} \sum_{i=1}^n (q_{e, \text{meas}} - q_{e, \text{calc}})^2} \quad \dots (3)$$

The experimental results revealed that the values of RMSE in the Langmuir isotherm were lower than that obtained by using the other models, confirming that the Langmuir isotherm better represented the adsorption of cyanide onto NBAC. These data suggested that the adsorption of cyanide occurred on a monolayer (the adsorbed layer is one molecule in thickness), as assumed in the formulation of the Langmuir model for an NBAC surface. This experimental data were in agreement with most of the other available data (Table 1). A dimensionless separation factor or equilibrium constant  $R_L$ <sup>30</sup>, expressed as  $R_L = 1/(1 + K_L C_0)$ , was used for further evaluating the favorable Langmuir model. The value of  $R_L$  indicates the adsorption situations to be either unfavorable ( $R_L > 1$ ), linear ( $R_L = 1$ ), favorable ( $0 < R_L < 1$ ), or irreversible ( $R_L = 0$ ). Based on the Langmuir constant, the value of this parameter ( $R_L$ ) for cyanide adsorption with NBAC falls between 0 and 1, which confirms that cyanide adsorption is favorable under the selected conditions of this study. Moreover, it is known that  $1/n$  in the Freundlich model is the adsorption intensity and the values of  $1/n$  determine whether the isotherm is irreversible ( $1/n = 0$ ), favorable ( $0 < 1/n < 1$ ), or unfavorable ( $1/n = 1$ )<sup>30</sup>. According to the results shown in Table 4, the  $1/n$  value of the Freundlich isotherm was in the range of 0.38 to 0.46 at different solution temperatures, which revealed that cyanide was favorably adsorbed onto NBAC. Table 4 indicates that the Temkin isotherm ( $R^2 = 0.942$  to  $0.952$ ) was a good fit for the adsorption of cyanide onto NBAC. Further, on the basis of the information given in Table 4, the Temkin adsorption potential ( $B_T \ln A_T$ ) of NBAC was determined and was in the range of 8.23 to 35.36 kJ/mol at solution temperatures between 24 and 50 °C, and the fact that it was greater than 8 kJ/mol confirmed that the bonding of cyanide ions

onto the NBAC surface was very strong. Isotherm experimental data were further interpreted by using the D–R isotherm to distinguish between physical and chemical adsorption. An analysis of the data with the D–R model revealed that the energy (calculated by  $E = 1/\sqrt{2K_{DR}}$ ) required by the cyanide adsorption onto NBAC was in the range of 8.5 to 15.8 kJ/mol. The values of  $E$  indicated that the mean adsorption free energy was one mole of the adsorbent when it was transferred to the surface of the adsorbent from the aqueous phase in the solution, which led to the conclusion that the adsorption mechanism was an ion-exchange or chemisorption process.

As given in Table 4, the values of  $E$  are in the typical range of bonding energy for chemisorption (8–16 kJ/mol)<sup>35</sup>, which demonstrates that in the adsorption of cyanide onto NBAC, ion exchange and chemisorption play a significant role. These data reconfirm the result obtained from the pH and FTIR studies and will be discussed in detail in the section on kinetic studies. The maximum adsorption capacity ( $q_{max}$ ) of cyanide onto NBAC was 102.5 mg/g for 24°C (Table 4), which is better than that of the other adsorbents that have been tested for the adsorption of cyanide (Table 1). From this observation, it can be suggested that cyanide was favorably adsorbed onto NBAC and that NBAC is a suitable adsorbent because of their high adsorption capacity, their abundant availability at very low costs, and their economic adsorbence for the uptake of cyanide from industrial wastewater.

#### Kinetic adsorption modeling

Kinetic adsorption is perhaps the most important factor in adsorption system design when determining the adsorbent uptake rate<sup>36</sup>. Therefore, to investigate the adsorption mechanism of cyanide removal, the experimental data were fitted with the most commonly used pseudo first- and second-order kinetics model under the different experimental conditions given in Table 2 (Run 5). The pseudo first-order-kinetic linear equation is generally expressed as follows:

$$\ln(q_{e, \text{meas}} - q_t) = \ln(q_{e, \text{calc}}) - k_1 t \quad \dots (4)$$

The linear regression analysis of  $\ln(q_{e, \text{meas}} - q_t)$  vs.  $t$  for different experimental conditions will give the value of  $q_{e, \text{calc}}$  ( $q_{e, \text{calc}} = \exp(\text{intercept})$ ) and  $k_1$  ( $k_1 = -\text{slope}$ )<sup>21</sup>.

The pseudo second-order kinetic linear equation is generally expressed as follows:

$$\frac{t}{q_t} = \frac{1}{k_2 q_{e,calc}^2} + \frac{1}{q_{e,calc}} t \quad \dots (5)$$

The value of  $q_{e,calc}$  ( $q_{e,calc} = 1/\text{slope}$ ) and  $k_2$  as the rate constant ( $k_2 = \text{slope}^2/\text{intercept}$ ) of the pseudo second-order equation can be obtained from a linear regression analysis of  $t/q_t$  vs.  $t$ . The applicability of the fitted model was selected with a comparison of the correlation coefficient. The analyses of the data using first-order and second-order kinetic models for all the three investigated concentrations indicated that cyanide adsorption on NBAC followed the pseudo second-order kinetic model with higher determination coefficients than those of the pseudo first-order model (Table 5). Apart from the correlation coefficient ( $R^2$ ) in the kinetics studies, the validity of the kinetic models for the adsorption data was further evaluated by calculating the average relative error (ARE), the sum of squares error (SSE), and the average percentage error (APE)<sup>34</sup>, which can be expressed as (Eqs. 6-8):

$$\text{ARE} = \sum_{i=1}^N \left[ \frac{q_{e,meas} - q_{e,calc}}{q_{e,meas}} \right]_i \quad \dots (6)$$

$$\text{SSE} = \sum_{i=1}^N (q_{e,calc} - q_{e,meas}) \quad \dots (7)$$

$$\text{APE} = \sum_{i=1}^N \left[ \frac{(q_{e,meas} - q_{e,calc})}{q_{e,meas}} \right]_i \times 100 \quad \dots (8)$$

Table 5 present the kinetic information obtained from the pseudo first- and pseudo second-order models. Further evaluation of the experimental data given in Table 5 indicated that the ARE, SSE, and APE values for all three investigated concentrations in the case of the pseudo second-order model are lower than those in the case of the pseudo first-order model, which implies that the pseudo second-order kinetic model provides excellent fitness for the adsorption of cyanide onto NBAC for the three studied initial cyanide concentrations. The results demonstrated that chemical adsorption likely controlled the adsorption of cyanide onto the NBAC, which may imply the valence forces via sharing or an exchange of electrons between cyanide and NBAC<sup>36</sup>. Moreover, as shown in the kinetic data given in Table 5, the calculated

adsorption capacity ( $q_{e,calc}$ ) in the case of the pseudo second-order model was very close to the experimental adsorption capacity ( $q_{e,meas}$ ) under selected conditions, which confirms the high correlation of experimental data to the pseudo second-order model. Further, the adsorption capacity, with an increase in the initial concentration, increased, revealing that the resistance to the cyanide adsorption from solution bulk onto NBAC was reduced by the mass transfer driving force. Third, Table 5 lists the values of  $k_2$  as the pseudo second-order adsorption constant under similar experimental conditions as 0.052, 0.006, and, 0.004 for the initial cyanide concentrations of 100, 200, and 300 mg/L, respectively. As shown,  $k_2$  values decreased with an increase in the cyanide concentration. This trend demonstrates that the mass transfer driving force probably increased and the rate improved with an increase in the initial concentration gradient<sup>37</sup>. The data given in Table 1 indicates that most of the previous works also reported that the pseudo second-order kinetics best fit the models with respect to the adsorption of cyanide onto different adsorbents.

The removal of target contaminates by adsorption processes involves a number of steps, each of which can affect the rate of adsorption. There is a possibility that bulk solution transport (boundary layer), external (film) resistance to transport, and internal (pore) transport will be the rate-limiting steps in the adsorption of a solute onto an adsorbent. The transport steps occur in a series and are most likely slow processes called the rate-limiting steps, which control the rate of adsorption<sup>26</sup>. The most commonly tested pore diffusion model, proposed by Weber and Morris, was also applied for evaluating the experimental adsorption kinetics data. The linear form of the equation is as follows (Eq. 9):

$$q_t = k_{id} t^{0.5} + C \quad \dots (9)$$

The constant of  $k_{id}$  was obtained from the slope of the plot of  $q_t$  against  $t^{0.5}$  (Ref.33). The plot of intraparticle diffusion may present multi-linearity correlations, which show that two or more steps were possibly involved in the adsorption process. The intraparticle diffusion model plots for the adsorption of all cyanide samples (concentration: 100, 200, and 300 mg/L) onto the NBAC are shown in Fig. 6. Figure 6 shows two linearity shapes for three concentrations, which confirms that different adsorption mechanisms (film and intraparticle

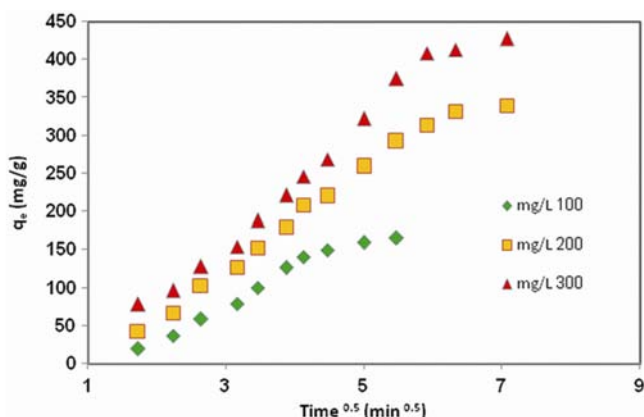


Fig. 6 — Intraparticle diffusion model plot for the adsorption of cyanide onto NBAC

diffusion) are involved in the adsorption of cyanide onto NBAC. The initial portion of the plots indicates that the boundary layer diffusion probably limited the cyanide adsorption, whereas the second portion occurrences caused by intraparticle or pore diffusion were the adsorption-limiting step. The parameters obtained from the intraparticle diffusion model with different initial cyanide concentrations are specified in Table 5. These results indicated that when the initial cyanide concentration increased from 100 to 300 mg/L, the rate constant ( $k_{id}$ ) of adsorption increased from 0.928 to 3.714 under similar experimental conditions, which confirms the experimental reduction in  $k_2$  and the increase in the rate of adsorption as a function of the initial concentration. The values of  $C$ , intercept of the Weber- Morris model, provide information about the thickness of the film of water around the adsorbent particles<sup>38</sup>. Table 5 reveals that the value of  $C$  was positive and increased with an increase in the cyanide concentration, indicating that film diffusion occurred on the cyanide–NBAC interface. Another important point found in Fig. 6 is that the plots of  $q_t$  vs.  $t^{0.5}$  did not pass through the origin, indicating that intraparticle diffusion was not a rate-controlling step for the cyanide adsorption onto NBAC. From this observation, it can be suggested that film and intraparticle diffusion were concurrently operating during the adsorption of cyanide from the solution bulk onto the NBAC.

#### Thermodynamic study

An analysis of the thermodynamic data reveals important information about the mechanism of the adsorption process. To explain and confirm the mechanism of cyanide adsorption onto NBAC, the

thermodynamics parameters associated with the adsorption were determined under conditions given in Table 2 (Run 6) by using Eqs. 10-12:

$$\Delta G^\circ = -RT \ln K. \quad \dots(10)$$

$$K_o = \frac{q_e}{C_e} \quad \dots(11)$$

$$\ln K_o = -\frac{\Delta H^\circ}{RT} + \frac{\Delta S^\circ}{R} \quad \dots(12)$$

The values of  $\Delta H^\circ$  and  $\Delta S^\circ$  were calculated from the slope and the intercept of a plot of  $\ln K_o$  against  $1/T$ , respectively<sup>33,39</sup>. The thermodynamic data indicated that  $\Delta G^\circ$  (standard free energy changes) sorption values were negative at all the considered temperatures, which are outside the range of physical adsorption ( $-20$  to  $0$  kJ/mol)<sup>40</sup>. These experimental data suggest that the adsorption of cyanide onto NBAC is spontaneous and enhanced by the affected chemical. The positive value of the enthalpy of the present experiment confirmed the endothermic nature of the adsorption process. The values of enthalpy change ( $+31.45$  to  $+73.766$  kJ/mol) higher than  $29$  kJ/mol imply that the chemisorption may be responsible for cyanide adsorption onto NBAC<sup>39</sup>. Moreover, the positive and high value of entropy indicates that NBAC has a high affinity for the adsorption of cyanide<sup>37</sup>. Thus, these data demonstrate that adsorption is endothermic and confirmed the dominance of the chemisorption mechanism of the cyanide adsorption onto NBAC. Thus, the results of the thermodynamic analysis reconfirmed the theory of the chemisorption of cyanide onto NBAC.

#### Treatment of electroplating plant wastewater by NBAC

Upon the completion of the basic adsorption experiments, the efficacy of NBAC in the removal of cyanide from industrial wastewater was tested under the conditions given in Table 2. For this, a bulk wastewater sample was obtained from a local electroplating plant. The cyanide, pH, BOD<sub>5</sub> and chromate concentration of collected wastewater was determined at the beginning of adsorption experiments, where values of 112 mg/L, 8.3, 147 mg/L, and 22.4 mg/L, respectively, were obtained. The test was conducted at the pH level of the original wastewater. A relatively low amount of NBAC (1.25 mg/L) at a relatively short contact time (40 min) could remove most of the cyanide ( $> 99\%$ ) to ensure

that the cyanide concentration in the treated water was well below the standard level for the discharge of wastewater into surface waters<sup>2</sup>. Further, it improved some of the other characteristics such as chromate and BOD<sub>5</sub> of the treated wastewater. Thus, NBAC is an efficient adsorbent for the removal of cyanide from industrial wastewaters.

### Conclusion

In this study, activated carbon is prepared from agricultural waste using an innovative NH<sub>4</sub>Br-soaked activation method (NBAC) and its adsorption potential is evaluated. It is found that the adsorption rate of cyanide onto NBAC depends on the solution pH level, NBAC quantity, contact time, and the initial cyanide concentration. A considerable amount of cyanide could be adsorbed onto 1.25 mg NBAC within a short contact time of 40 min. The pseudo-second order is a suitable fit with the kinetic data. The maximum adsorption capacity calculated from the Langmuir isotherm, the best fit model to the experimental data, is 102, 109 and 117 mg/g at temperatures of 24, 35 and 50°C, respectively. The results reveal that the rate of adsorption is controlled by the interparticle diffusion and chemisorption. Further, NBAC reduces the concentration of cyanide in industrial wastewater to levels below the designated standard for effluent discharge into surface waters. In brief, it can be concluded that NBAC has a high adsorption affinity toward cyanide, making the NBAC adsorption process a viable and potential process for the treatment of wastewater containing this contaminant.

### Nomenclature

$A_T$	Temkin isotherm equilibrium-binding constant (L/g)
$B_{DR}$	D-R isotherm constant ( $\text{mol}^2/\text{kJ}^2$ )
$B_T$	Tempkin isotherm constant (mg/g)
$C_0$	Cyanide initial concentration (mg/L)
$C_e$	Equilibrium concentration (mg/L)
$C_t$	Cyanide concentrations at a time t (mg/L)
$E$	Free energy (kJ/mol)
$K_e$	Thermodynamic equilibrium constant
$k_1$	Pseudo-first order rate constant (1/min)
$k_2$	Pseudo-second order rate constant (mg/g min)
$K_{id}$	Constant of intraparticle diffusion ( $\text{mg/g min}^{0.5}$ )
$K_L$	Langmuir isotherm constant (L/mg)
$m$	Mass of NBAC (g)
$\text{pH}_{zpc}$	pH of zero point charge

$q_e$	Amount of cyanide adsorbed per gram of NBAC at equilibrium (mg/g)
$q_{e,calc}$	Calculated $q_e$ value (mg/g)
$q_{e,meas}$	Experimentally measured $q_e$ value (mg/g)
$q_{max}$	Maximum amount of cyanide adsorbed per gram of NBAC (mg/g)
$q_t$	Adsorption capacity at time t (mg/g)
$R$	Universal gas constant (8.314 J/mol K)
$t$	Time of contact (min)
$V$	Volume of the cyanide solution (L)
$\Delta G^\circ$	Gibbs energy change (kJ/mol)
$\Delta H^\circ$	Standard enthalpy change (kJ/mol)
$\Delta S^\circ$	Standard entropy change (kJ/mol.K)

### Acknowledgement

The authors express their sincere gratitude to the Bushehr University of Medical Sciences for providing the technical and financial support for this study.

### References

- Sirianuntapiboon S & Chuamkaew C, *Bioresource Technol.*, 98 (2) (2007) 266.
- Dash R R & Gaur A, *J Hazard Mater*, 163 (1) (2009) 1.
- Campos M G, Pereira P & Roseiro J C, *Enzyme Microb Technol.* 38 (2006) 848.
- Department of Interior U S, Cyanide Fact Sheet Bureau of Reclamation, Technical Service Center: Water Treatment Engineering and Research Group, (2001) 1.
- Dash R R, BaloMajumder C & Kumar A, *Chem Eng J*, 146 (2009) 408.
- Noroozifar M, Khorasani-Motlagh M & Ahmadzadeh Fard P, *J Hazard Mater*, 166 (2009) 1060.
- White D M, Pilon T A & Woolard C, *Water Res*, 34 (2000) 2105.
- Sirianuntapiboon S, Chairattanawan K & Rarunroeng M, *J Hazard Mater*, 154 (2008) 526.
- Kaewkannetra P, Imai T, Garcia-Garcia F J & Chiu T Y, *J Hazard Mater*, 172 (2009) 224.
- EPA, *Technical report: Treatment of cyanide heap leaches and tailings*, U S Environmental Protection Agency, Office of Solid Waste, Washington, DC (1994) (EPA530R94037, PB94201837).
- Chen C Y, Kao C M & Chen S C, *Chemosphere*, 71 (2008) 133.
- Kao C M, Liu J K, Lou H R, Lin C S & Chen S C, *Chemosphere*, 50 (2003) 1055.
- Watanabe A, Yano K, Ikebukuro K & Karube I, *Microbiology*, 144 (1998) 1677.
- Aksu Z & Tunc O, *Process Biochem*, 40 (2005) 831.
- Moussavi G, Alahabadi A, Yaghmaeian K & Eskandari M, *Chem Eng J*, 217 (2013) 119.
- Rivera-Utrilla J, Prados-Joya G, Sanchez-Polo M, Ferro-Garcia M A & Bautista-Toledo I, *J Hazard Mater*, 170 (2009) 298.
- Deveci H, Yazıcı E Y, Alp I & Uslu T, *Int J Miner Process*, 79 (2006) 198.
- Monser L & Adhoum N, *Sep Purif Technol*, 26 (2002) 137.

- 19 Adhoum N & Monser L, *Chem Eng Process*, 41 (2002) 17.
- 20 Dai X, Jeffrey M I & Breuer P L, *Hydrometallurgy*, 101 (2010) 99.
- 21 Behnamfard A & Salarirad M M, *J Hazard Mater*, 170 (2009) 127.
- 22 Depci T, *Chem Eng J*, 181-182 (2012) 467.
- 23 Chang Q, Lin W & Ying W, *J Hazard Mater*, 184 (2010) 515.
- 24 Altenor S, Carene B, Emmanuel E, Lambert J, Ehrhardt J J & Gaspard S, *J Hazard Mater*, 65 (2008) 1029.
- 25 APHA, *Standard Methods for the Examination of Water and Wastewater*, 20 th edn (1998).
- 26 Wahab M A, Jellali S & Jedidi N, *Biores Technol*, 101 (2010) 5070.
- 27 Elliott H A & Huang C P, *Water Res*, 15 (1981) 849.
- 28 Barakat M A, *J Colloid Interface Sci*, 291 (2005) 345.
- 29 Moussavi G & Khosravi R, *J Hazard Mater*, 183 (2010) 724.
- 30 Asgari G, Ramavandi B & Farjadfard S, *Scientific World Journal*, 1-10 (2013) 2013.
- 31 Guo R, Chakrabarti C L, Subramanian K S, Ma X, Lu Y, Cheng J & Pickering W F, *Water Environ Res*, 65 (1993) 640.
- 32 White D M, Pilon T A & Woolard C, *Water Res*, 34 (2000) 2105.
- 33 Khademi Z, Ramavandi B & Ghaneian M T, *J Environ Chem Eng*, 3 (2015) 2057.
- 34 Foo K Y & Hameed B H, *Chem Eng J*, 156 (2012) 1.
- 35 Asgari G, Ramavandi B, Rasuli L & Ahmadi M, *Desal Water Treat*, (2013). doi: 10.1080/19443994.2013.769928.
- 36 Hameed B H, Tan I A W & Ahmad A L, *Chem Eng J*, 144 (2008) 235.
- 37 Aydın Y A & Aksoy N D, *Chem Eng J*, 151 (2009) 188.
- 38 E l Nemr A, *J Hazard Mater*, 161 (2009) 132.
- 39 Duranoglu D, Trochimczuk A W & Beker U, *Chem Eng J*, 187 (2012) 193.
- 40 Jai Poinerna G E, Malay G K, Ng Y J, Touma I B, Anand S & Singh P, *J Hazard Mater*, 185 (2011) 29.